PROCEEDINGS B

rspb.royalsocietypublishing.org

Research

Cite this article: Tulenko FJ, Massey JL, Holmquist E, Kigundu G, Thomas S, Smith SME, Mazan S, Davis MC. 2017 Fin-fold development in paddlefish and catshark and implications for the evolution of the autopod. *Proc. R. Soc. B* **284**: 20162780. http://dx.doi.org/10.1098/rspb.2016.2780

Received: 20 December 2016
Accepted: 24 April 2017

Subject Category:
Development and physiology

Subject Areas:
developmental biology, evolution, palaeontology

Keywords:
HoxA, AER, fin-fold, paddlefish, catshark, autopod

Author for correspondence:
Marcus C. Davis
e-mail: mdavi144@kennesaw.edu

Electronic supplementary material is available online at rs.figshare.com.

THE ROYAL SOCIETY PUBLISHING

Fin-fold development in paddlefish and catshark and implications for the evolution of the autopod

Frank J. Tulenko[1,2], James L. Massey[3], Elishka Holmquist[1], Gabriel Kigundu[1], Sarah Thomas[1], Susan M. E. Smith[1], Sylvie Mazan[4] and Marcus C. Davis[1]

[1]Department of Molecular and Cellular Biology, Kennesaw State University, GA 30144, USA
[2]Australian Regenerative Medicine Institute, Monash University, Victoria, 3800, Australia
[3]Department of Ecology and Evolutionary Biology, University of Colorado Boulder, CO 80309, USA
[4]CNRS, Sorbonne Universités, UPMC Univ Paris 06, UMR7232, Observatoire Océanologique, F-66650 Banyuls-sur-Mer, France

FJT, 0000-0003-3142-3551; MCD, 0000-0002-2462-0138

The evolutionary origin of the autopod involved a loss of the fin-fold and associated dermal skeleton with a concomitant elaboration of the distal endoskeleton to form a wrist and digits. Developmental studies, primarily from teleosts and amniotes, suggest a model for appendage evolution in which a delay in the AER-to-fin-fold conversion fuelled endoskeletal expansion by prolonging the function of AER-mediated regulatory networks. Here, we characterize aspects of paired fin development in the paddlefish *Polyodon spathula* (a non-teleost actinopterygian) and catshark *Scyliorhinus canicula* (chondrichthyan) to explore aspects of this model in a broader phylogenetic context. Our data demonstrate that in basal gnathostomes, the autopod marker *HoxA13* co-localizes with the dermoskeleton component *And1* to mark the position of the fin-fold, supporting recent work demonstrating a role for *HoxA13* in zebrafish fin ray development. Additionally, we show that in paddlefish, the proximal fin and fin-fold mesenchyme share a common mesodermal origin, and that components of the Shh/LIM/Gremlin/Fgf transcriptional network critical to limb bud outgrowth and patterning are expressed in the fin-fold with a profile similar to that of tetrapods. Together these data draw contrast with hypotheses of AER heterochrony and suggest that limb-specific morphologies arose through evolutionary changes in the differentiation outcome of conserved early distal patterning compartments.

1. Introduction

The transition from fins to limbs during the tetrapod invasion of land is one of the compelling puzzles in comparative anatomy, and provides a paradigm for exploring the relationship between skeletal development and anatomical novelty in a macro-evolutionary context [1,2]. The paired fins of gnathostomes contain two types of structural supports, a series of endoskeletal radials proximally, and a dermoskeleton consisting of connective tissue (e.g. actinotrichia/ceratotrichia) and fin rays, distally. Sarcopterygian fossils record both the gradual elaboration of distal fin endoskeletons (e.g. *Sauripterus* [3]), as well as a reduction in the relative size of the dermoskeleton (e.g. *Tiktaalik* [4]) before its complete loss in the first limbs (e.g. *Acanthostega* [5]). Interestingly, fossils such as *Sauripterus* demonstrate substantial overlap between the dermal rays and endoskeleton, a tissue distribution considered problematic in the context of current developmental models for fin-limb evolution [2,6].

Over the past several decades, the integration of fossil and molecular datasets has provided new insights into appendage evolution (e.g. [2,7–9]), with a particular focus on Hox family transcription factors and their role in proximo-distal patterning of the endoskeleton [10–14]. In tetrapods, limbs form as outgrowths of body wall lateral plate mesoderm (LPM) and overlying ectoderm, ultimately

giving rise to a morphologically regionalized series of bones, the stylopod, zeugopod and autopod. During this process, *HoxA* and *HoxD* cluster genes are expressed in early and late phases [15] regulated by enhancer topology domains outside the cluster [14,16,17]. Of these genes, *HoxA11* and *HoxA13* have emerged as molecular markers for the regions of the limb bud that give rise to the zeugopod and autopod, respectively [18–20]. *Meis* expression marks the position of the stylopod in response to proximalizing signals from the trunk [21–25], though the specific mechanisms underlying Meis and Hox boundary formation remain actively investigated [26].

The regulatory networks that integrate limb bud outgrowth and patterning have been partially characterized in mouse and chick, revealing key molecular interactions between the posterior limb bud mesenchyme (i.e. the zone of polarizing activity, ZPA) and the distal limb bud ectoderm (the apical ectodermal ridge, AER) [27,28]. In one pathway, Sonic Hedgehog (Shh) from the ZPA induces expression of the Bmp-antagonist *Gremlin*, which blocks Bmp inhibition of *Fgf* expression in the AER. In turn, Fgfs from the AER maintain ZPA-Shh, propagating a feedback loop that terminates with digit chondrogenesis [29–37]. Interestingly, recent work in mice demonstrates that LIM-homeodomain transcription factors mediate Shh induction of *Gremlin*, and integrate this pathway with a second positive feedback loop between mesenchymal Fgf10 and AER-Fgfs [38]. Components of both of these pathways are expressed within the autopod-forming field and are required for expansion of the limb bud primordia and proper patterning of the digits [27,28].

One of the keys to understanding the fin-to-limb transition is gaining insight into how ancestral gene networks were modified to give rise to limb-specific morphologies. Unlike tetrapods, in cartilaginous and bony fishes the endoskeleton articulates with a dermal skeleton, which provides structural support for the distal fin-fold. To date, the early development of the dermal skeleton has been primarily studied in teleosts [9,39–42]. These studies indicate that in early fin buds, the distal ectoderm thickens and gives rise to a short apical fold (AF) that is histologically [41] and molecularly [43] similar to the tetrapod AER. The AF then elongates to form the fin-fold proper, which opens proximally to create a transient extracellular space where the first connective tissue components of the dermal skeleton, the actinotrichia, are deposited. Shortly thereafter, mesenchymal cells from the proximal fin migrate along the actinotrichia to populate the fin-fold [41], a process that has been shown to require *Actinodin* (an actinotrichia component [9]) and AER infiltration by somitic cells [44].

Morphogenetic differences between the formation of limbs and teleost paired fins provide the embryological context for current models of the fin-to-limb transition. According to Thorogood's [45] influential 'clock' model, delays in the conversion of the AER to a fin-fold prolong the signalling influence of the AER on the endoskeletal mesenchyme, resulting in an expansion of the fin radials and a reduction of the dermoskeleton. Limbs, which lack a dermoskeleton, reflect the extreme of this hypothesis in that the AER persists through autopod formation, never giving rise to a fin-fold. While Thorogood's original model was morphogenetic, the conceptual framework it introduced (i.e. a heterochronic shift in the relative timing of AER-to-fin-fold conversion) remains a key aspect of more recent models of appendage evolution that incorporate molecular datasets [2,12,46–48]. In these molecular models, *Meis* and *HoxA/D* transcription factors regionalize the endoskeletal mesenchyme, but are absent from the fin-fold, which is treated as a uniquely patterned module [13,14,49,50]; but see [51,52]. A recent functional study in zebrafish, however, has challenged this assumption, demonstrating that Cre-mediated labelling of cells with a history of activating the spotted gar HoxA enhancer e16 contribute to the fin-fold, and that fin rays fail to form in the absence of functional Hox13 paralogues [53]. Remarkably, these results provide evidence for a deep homology between the distal skeleton of finned and limbed vertebrates [53], though the phylogenetic distribution of HoxA13 expression relative to the dermal fin compartment of non-teleosts is unknown.

Herein, we characterize aspects of paired fin formation in the basal actinopterygian *Polyodon spathula* (American paddlefish) and the chondrichthyan *Scyliorhinus canicula* (lesser spotted catshark) to evaluate models of fin-limb evolution in a broader phylogenetic context and to better understand fin-fold ontogeny. Our new data reveal that *HoxA13* expression marks the position of the fin-fold, providing evidence that this feature is plesiomorphic to gnathostomes. Additionally, in paddlefish we show that the mesenchyme of the proximal fin and fin-fold share a common embryonic origin, and that components of the Shh/LIM/Gremlin/Fgf transcriptional network critical to distal limb formation are expressed in the fin-fold with a profile similar to that of tetrapods. Together, these data support an early developmental similarity between the fin-fold and autopod [53], and suggest that AER-mediated regulatory networks may be maintained following fin-fold formation. We propose a scenario for gnathostome appendage evolution in which limb-specific morphologies arose through changes in the differentiation outcomes of conserved early proximo-distal patterning domains.

2. Material and methods

(a) Animals

Embryos of *P. spathula* were obtained from Osage Catfisheries Inc. (Osage Beach, MO, USA), raised in 18°C freshwater tanks, fixed in Carnoy's solution, and stored in 100% ethanol at −20°C. Embryos of *S. canicula* were obtained from Roscoff Marine Station (France), raised in 17°C seawater, fixed in 4% PFA, and stored in 100% methanol at −20°C. Staging according to [54–56].

(b) Cloning

Paddlefish cDNA was generated according to [52], and primers were designed based on transcriptome sequences ([57]; electronic supplementary material, table S1). PCR products were cloned into pGEM-T Easy (Promega) and sequenced (Genscript). Protein sequences, and homologues identified via BLAST, were aligned with MUSCLE [58] and alignments trimmed with trimAl [59]. Orthology was confirmed by BIONJ [60] neighbour joining analysis (electronic supplementary material, figure S1 and S2).

(c) *In situ* hybridization and immunohistochemistry

For *in situ* hybridizations, full PCR products obtained from primer sets were used for probe synthesis according to [52]. Single and double *in situs* were performed as described in [52,61], respectively. Sense probe was used with stage-matched specimens as a negative control. For immunohistochemistry, embryos were cryosectioned following *in situ* hybridization, rinsed (PBS-Tw), blocked (5%NGS in PBS-Tw) and incubated in anti-skeletal muscle antibody 12–101 (DSHB; 1 : 20 in block). Sections were rinsed, incubated in HRP-conjugated goat anti-mouse IgG (H + L) (Life Technologies), rinsed again, and developed using an SK-4100 peroxidase substrate

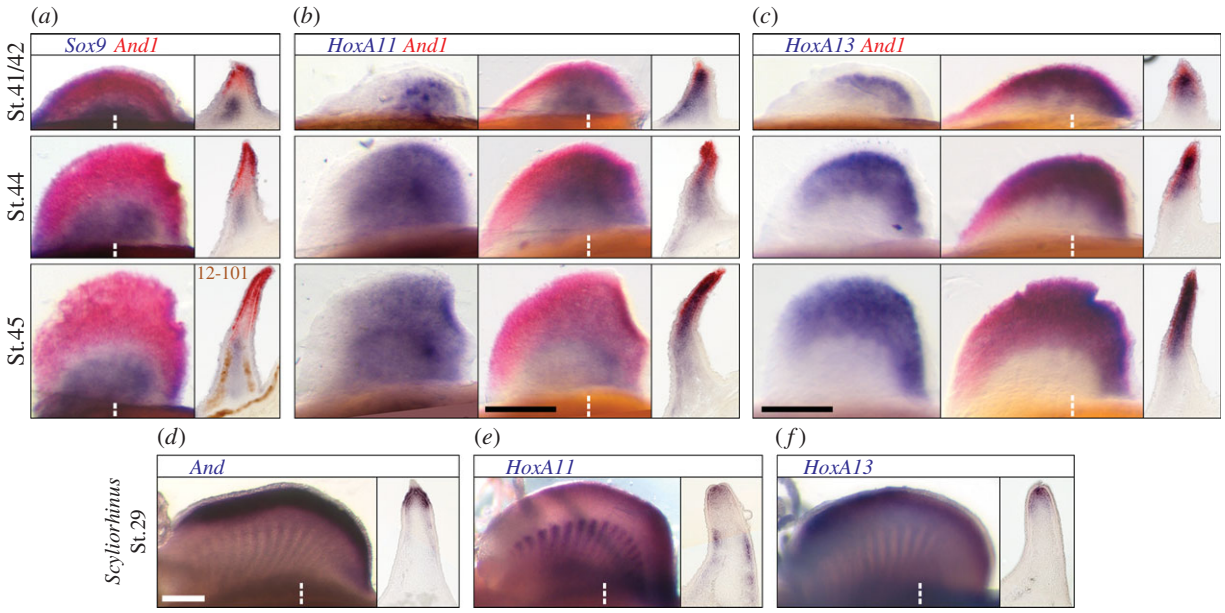

Figure 1. *5′ HoxA* expression for paddlefish (*a–c*) and catshark (*d–f*). (*a*) Double *in situ* for *Sox9* (blue)+*And1* (red). Stage 45 skeletal muscle labelled with 12-101 (brown). (*b*) *HoxA11* and *HoxA11* (blue)+*And1 (red)*. (*c*) *HoxA13* and *HoxA13* (blue)+*And1* (red). (*d–f*) *In situ* for *And1* (*d*), *HoxA11* (*e*) and *HoxA13* (*f*) in catshark. Whole fins: ventral view, anterior is left. Cross sections: ventral is left. Dashed lines: approximate plane of section. Scale bars, 200 µm.

kit (Vector labs). Whole mount imaging was done using a Zeiss Discovery.V12 Stereo microscope with AxioCam MRc5 camera.

(d) DiI labelling

DiI injections were performed as described in [62]. Somite and nephric duct margins were used as landmarks to target LPM. Injected embryos were photographed at time of injection (Stage 23/24), raised to Stage 43/44, and fixed in 4% PFA. Embryos with the brightest fluorescence were cryosectioned, counter-stained with Phalloidin (1 : 200) and DAPI (1 : 10 000), and imaged using a Zeiss 710 Confocal Microscope.

(e) Histology

Cryosections were generated as described in [52]. Specimens were embedded in JB4-Plus (Polysciences), sectioned on a LKB-8801 ultra-microtome, stained with 0.5% Toluidine blue and imaged using a Zeiss AxioImager.M2 microscope with Axiocam 503 camera.

3. Results

In paddlefish, molecularly distinct endoskeletal and dermoskeletal compartments are established by the early fin-bud stage [52], presaging the ultimate arrangement of fin radials and actinotrichia in larvae [63]. In order to determine the tissue context for fin-fold patterning, we compared the labelling domains of the prechondrogenic marker *Sox9*, the fin-fold actinotrichia marker *And1*[9], and the skeletal muscle antibody 12–101 (figure 1*a*) with plastic-embedded cross sections through the pectoral fin (electronic supplementary material, figure S3). Consistent with a previous report in paddlefish, *Sox9* and *And1* were expressed by Stage 41 [52], making visible the cryptic boundary of the fin-fold mesenchyme and ectoderm proximal to the AF, as well as the position of endoskeletal condensations (figure 1*a*; electronic supplementary material, figure S3*d*). Significantly, *Sox9* and *And1* expression persisted through later stages (Stages 42–45), despite expansion of both compartments and the differentiation of the fin radial anlagen into cartilage (figure 1*a*; electronic supplementary material, figure S3*e–g*). By Stage 45, 12–101-positive myofibres were present in the dorsal and ventral muscle masses, aligning distally with the *Sox9*/*And1* boundary (figure 1*a*).

In tetrapods, the proximo-distally segregated expression domains of *Meis*, *HoxA11* and *HoxA13* mark the precursor regions of the limb bud that give rise to the stylopod, zeugopod and autopod, respectively [18–20]. Given the early specification of paddlefish fin buds into endoskeletal and dermoskeletal compartments—and the highly mesenchymal nature of the fin-fold in cross section—we next characterized the expression of *Meis2*, *HoxA11* and *HoxA13* to determine if these genes segregated with *And1* patterning boundaries and morphological regionalization of the skeleton. In stage 42–45 pectoral fins, transcripts of *Meis2* were restricted to the anterior and posterior proximal mesenchyme (electronic supplementary material, figure S3). At these stages, *HoxA11* expression overlapped with *Meis2* posteriorly and in section was continuous between the mesenchyme of the proximal fin and *And1*-positive fin-fold in the posterior part of the fin (figure 1*b*). By contrast, *HoxA13* expression was distally restricted, nesting within the broader domain of *HoxA11* (figure 1*b*,*c*). Strikingly, the proximal boundary of *HoxA13* expression aligned with that of *And1* (figure 1*c*).

The co-localization of *HoxA13* and mesenchymal *And1* indicates a patterning similarity between the fin-fold of paddlefish and the autopod, despite differences in the differentiation outcome of these distal appendage compartments. In order to test the antiquity of this feature, we extended our analysis of *5′HoxA* and *And1* expression to the catshark as a representative chondrichthyan. Previous work in catshark has shown that *And1* marks the position of the fin-fold in early fin buds [52], supporting a molecular similarity between the ceratotrichia of chondrichthyans and actinotrichia of actinopterygians. Consistent with this work, we observed *And1* expression in the distal fin ectoderm and mesenchyme of St. 29 pectoral fins (figure 1*d*). At this stage, *HoxA11* was expressed in the muscle buds extending from the base of the fin and the distal fin mesenchyme (figure 1*e*). By contrast, transcripts of *HoxA13* were exclusive to the distal fin mesenchyme,

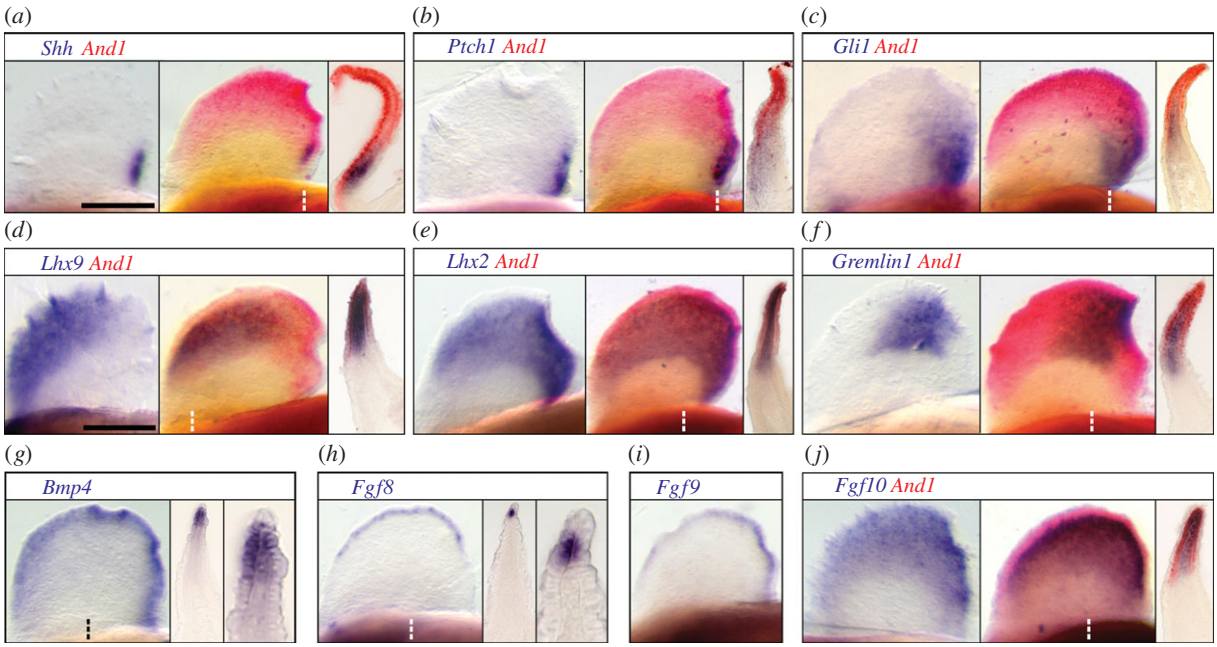

Figure 2. Paddlefish single and double (+ *And1*) *in situ* for Shh/Lim/Gremlin/Fgf transcriptional network components: *Shh* (*a*); *Ptch1* (*b*); *Gli1* (*c*); *Lhx9* (*d*); *Lhx2* (*e*); *Gremlin1* (*f*); *Bmp4* (*g*); *Fgf8* (*h*); *Fgf9(i);* and *Fgf10* (*k*) at Stage 44/45. (*g*,*h*) High magnification reveals expression in proximal AF (bracket) adjacent to the fin-fold mesenchyme, but not in distal AF. Whole fins: ventral view, anterior is left. Cross sections: ventral is left. Dashed lines: approximate plane of section. Scale bars, 200 µm.

forming a domain that in section roughly aligned with that of both *HoxA11* and *And1* (figure 1*f*). Together, these data support the overlap of *5′HoxA* genes in the distal fin (as in [64]), and demonstrate that in catshark, like paddlefish, *HoxA13* co-localizes with *And1*.

One prediction of heterochrony-based hypotheses for appendage evolution is that in finned vertebrates, the AER-to-AF conversion disrupts epithelial–mesenchymal signalling interactions that expand the Hox-patterned mesenchyme of the proximal fin [2,14,46,47,49]. In the lineage leading to tetrapods, retention of the AER at the expense of the fin-fold would have prolonged AER-mediated signalling, leading to an elaboration of the endoskeleton and, ultimately, the origin of digits. In paddlefish and catshark, the early specification of the fin-fold, and its conserved *HoxA13* identity with the autopod, together with functional data from zebrafish [53], challenge assumptions of fin-fold modularity and fuel the hypothesis that homologous AER-mediated regulatory networks may pattern the distal part of both fins and limbs. To test this hypothesis during fin-fold formation in paddlefish, we surveyed the expression of components of the Shh/LIM/Gremlin/Fgf transcriptional network critical to distal limb bud outgrowth and patterning [27,28,38].

Unexpectedly, in paddlefish transcripts of *Shh*, its receptors *Ptch1* and *Ptch2*, and the *Shh* response element *Gli1*, were detected within the *And1*-positive mesenchyme of the posterior fin-fold, suggesting a role for Shh in fin-fold patterning (figure 2*a–c*; electronic supplementary material, figure S5). Consistent with this result, predicted downstream components of the Shh/LIM/Gremlin/Fgf regulatory network were also expressed within the *And1* domain, forming a pattern similar to that observed in the distal limb bud. Of these genes, the LIM-homeodomain transcription factor *Lhx2* was posteriorly regionalized (figure 2*e*), overlapping with both the presumptive region of Shh signalling (figure 2*a–c*; electronic supplementary material, figure S5*a*) and *Gremlin1* (figure 2*f*), which formed a well-defined domain adjacent to the fin-fold 'ZPA'. Transcripts of *Bmp4*, a Gremlin inhibitory target, were detected along much of the distal fin-fold mesenchyme and ectoderm proximal to the AF (figure 2*g*). A larger region of mesenchymal *Bmp4* expression was detected posteriorly, aligning with the expression of *Tbx2* (electronic supplementary material, figure S5*b*), a *Gremlin* repressor and target of Bmp signalling in mouse limb buds [30]. In tetrapods, *Bmp4* as well as *Fgf4*, *Fgf8* and *Fgf9* mark the AER [65]. In paddlefish, these *Fgfs*, like *Bmp4*, were expressed in the proximal ectodermal cells of the AF directly adjacent to the fin-fold mesenchyme, but not is the distal AF (figure 2*h*,*i*; electronic supplementary material, figure S5*c*). Posteriorly, *Fgf9* expression extended to the base of the fin, overlapping the domains of *Lhx2*, *Gremlin1*, and *Shh* (figure 2*a–c*,*e*,*f*). As potential readouts of Fgf signalling, we also examined the ETS transcription factors *Etv4* and *Etv5*, as well as the retinoic acid degradation enzyme *Cyp26b1*, all markers of distal limb identity and downstream effectors of AER-Fgf signalling [66–68]. While *Etv4* was weakly expressed, both *Etv5* and *Cyp26b1* were strongly expressed in the fin-fold (electronic supplementary material, figure S5*d–f*).

During limb development, the Shh/LIM/Gremlin/Fgf regulatory loop functions in concert with epithelial-mesenchymal signalling between AER-Fgf8 and distal limb bud mesenchyme Fgf10, both of which continue to be expressed through autopod formation [69,70]. Notably, LIM homeodomain transcription factors also mediate this interaction, integrating patterning information along both the proximodistal and antero-posterior axes of the limb bud [38]. In paddlefish, transcripts of *Fgf10* were expressed throughout the fin-fold mesenchyme (figure 2*j*), co-localizing with the domains of *Lhx9* anteriorly and *Lhx2* posteriorly (figure 2*d*,*e*). In section, distal *Fgf10* expression directly abutted that of the AF-*Fgfs* (figure 2*j*), recapitulating the pattern in distal limbs.

In tetrapods, both the proximal (stylopod/zeugopod) and distal (autopod) bones of the limbs derive from LPM, and it is generally regarded that this is also the case for the fin radials of non-tetrapods. In order to test whether the mesenchyme

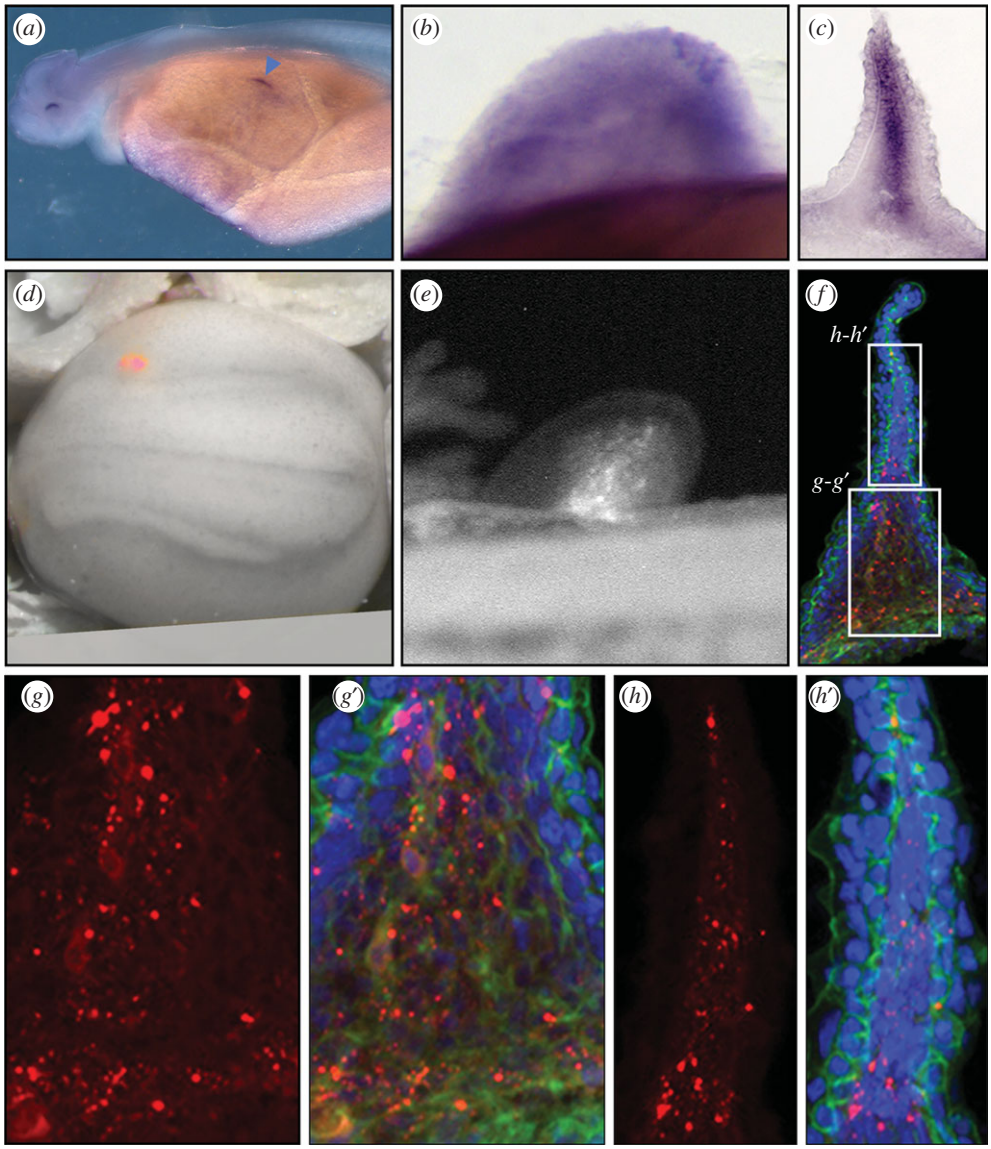

Figure 3. Paddlefish *in situs* for *Tbx5* at Stages 38 (*a*), and 43 (whole mount in (*b*), section in (*c*)) reveal expression in the LPM prior to fin-bud initiation (blue arrowhead in (*a*)) and persisting through outgrowth in both proximal fin and fin-fold. DiI labelling of LPM: (*d*) at time of injection (Stage 23); (*e*) pectoral fin (Stage 43); and cross sections (*f*–*h*′). Same embryo shown in (*d*–*h*′). Magnification reveals DiI in both proximal (*g*–*g*′) and distal fin (*h*–*h*′). Section (*h*–*g*′) counter-stained with phalloidin for cytoskeletal actin (green), DAPI for nuclei (blue).

of the proximal fin bud and fin-fold share a common LPM origin in paddlefish, we used a combined gene expression and vital dye fate-mapping approach. In jawed vertebrates, the T-box transcription factor *Tbx5* is expressed throughout the pectoral region and provides a molecular marker for the anterior LPM (e.g. catshark: [71]; zebrafish: [72]; chick: [73]). In paddlefish, *Tbx5* expression was present by Stage 38 in the earliest fin buds (figure 3*a*; electronic supplementary material, figure S6*a*,*b*) and persisted through later stages of outgrowth (figure 3*b*,*c*; electronic supplementary material, figure S6*c*–*f*). In Stage 43 cross sections, transcripts of *Tbx5* were detected throughout the region of *Sox9* expression proximally and *And1* distally, suggesting that both the endoskeletal and fin-fold mesenchyme derive from LPM (compare figures 1*a* and 3*d* and electronic supplementary material, figure S6*e*,*f*). To assess this directly, we used the lipophilic vital dye DiI to label the LPM of embryos shortly after gastrulation, prior to somitic cell emigration into the fins and body wall (Stage 23/24) (figure 3*d*; electronic supplementary material, figure S7). At this stage the margins of the somites and the nephric duct are visible (electronic supplementary material, figure S7*a*), providing mesodermal landmarks for LPM targeting. We then reared injected embryos ($n = 27$) to Stages 43/44 (figure 3*e*) and selected embryos with brightest labelling in the pectoral fin ($n = 15$) for sectioning ($n = 3$). Consistent with long-term *Tbx5* expression, DiI-positive cells were present throughout the proximal and fin-fold mesenchyme (figure 3*f*–*h*; electronic supplementary material, figure S7*b*,*c*), confirming that both tissues receive contributions from a common population of LPM. Dilution of labelling by cell division, however, precluded mapping the distribution of LPM in the mature anatomy of older larvae.

4. Discussion

Our characterization of *HoxA* expression in paddlefish refines previous data for this taxon [10,74] and demonstrates that transcripts of *HoxA13* co-localize with the actinotrichia protein *And1* in the fin-fold (figure 4*a*). We also show a similar overlap in catshark, indicating that *HoxA13* likely marked the patterning boundary of the early dermal skeleton in ancestral gnathostomes (figure 4*a*). These data, together with functional data demonstrating a role for Hox13 paralogues in zebrafish

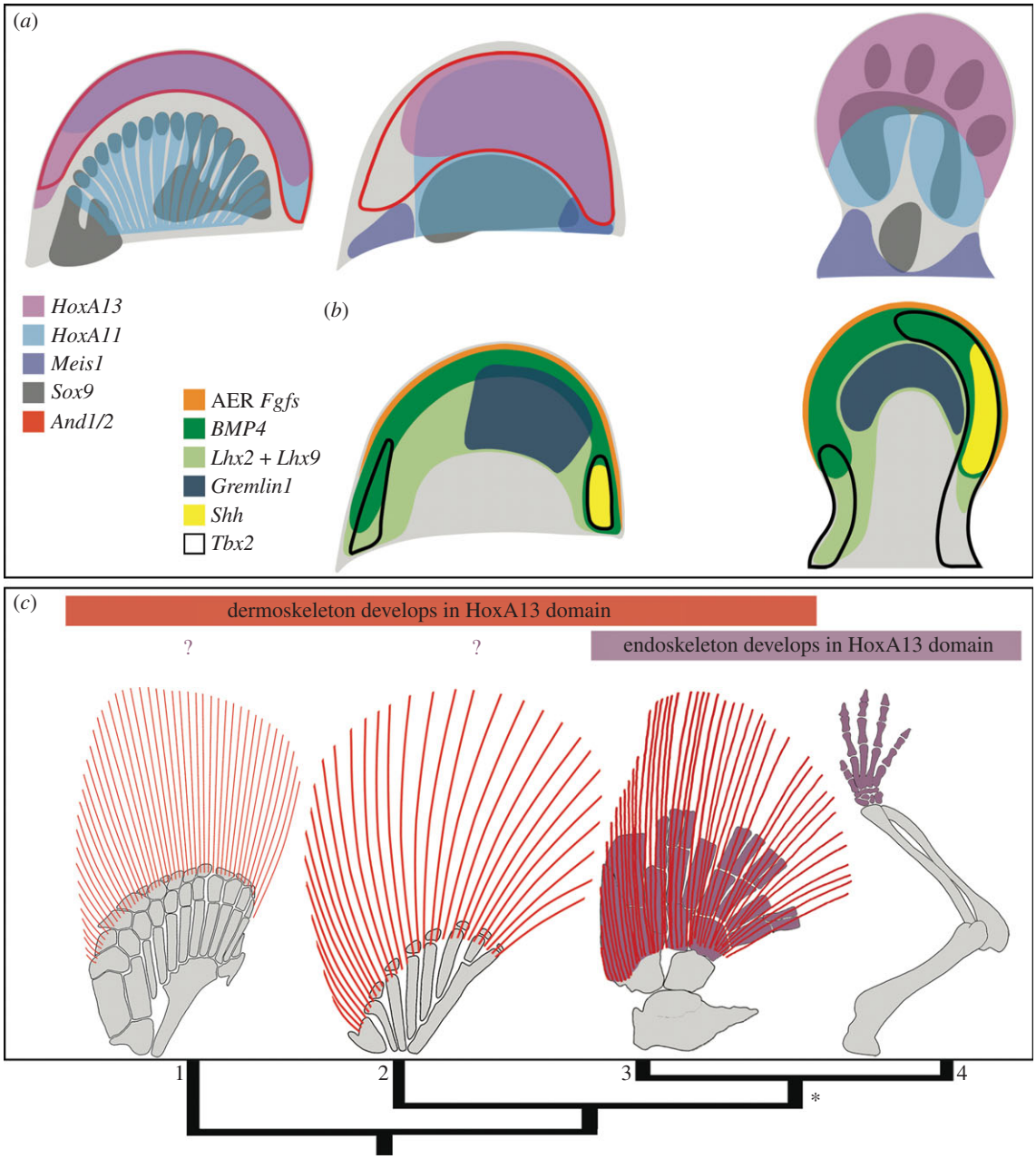

Figure 4. Developmental similarities with fin-folds suggest the autopod evolved through changes in the differentiation outcome of conserved early patterning domains. (*a*) *HoxA13* is expressed in the distal compartment of both fins (fin-fold) and limbs (autopod). (*b*) Shh/Lim/Gremlin/Fgf network components are expressed in the distal compartment of both fins and limbs, suggesting aspects of AER function are maintained in proximal AF cells. (*c*) Hypothesis for fin-limb evolution in which the autopod evolved through novel acquisition/expansion of chondrogenic competency in the distal compartment (*). In this scenario, dermal skeleton (red) and distal endoskeleton (purple) both reflect distinct differentiation outcomes of the *HoxA13* (pink from (*a*)) patterning domain. Overlap of dermal skeleton and distal endoskeletons seen in sarcopterygian fossils (3) may reflect this dual differentiation outcome, prior to complete loss of the dermal skeleton in tetrapods (4). 1, catshark; 2, paddlefish; 3, *Sauripterus*; 4, mouse. Catshark *Sox9* and E11.0-E11.5 mouse based on [8,18,23,30,38,75–77].

fin ray patterning, highlight flexibility in the differentiation outcome of Hox-patterned compartments across phylogeny [51–53]. Notably, the complete overlap between *HoxA13* and *HoxA11* expression in paddlefish and catshark is consistent with observations from teleosts [51,78], suggesting the reported negative effects of Hox13 proteins on distal *HoxA11* expression were acquired in the tetrapod lineage [79], likely through the evolution of a novel enhancer driving antisense transcript from the *HoxA11* locus [80]. While the modular nature of HoxA/D knockout phenotypes [15,53], *HoxD* regulatory switching in wrist formation [16] and stabilization of digit pentadactyly [80] all support the significance of Hox compartmentalization during limb development, the function of distal *Hox11* expression during fin development remains elusive.

The localization of *HoxA13* expression to the fin-fold and autopod indicates a developmental similarity between the morphologically regionalized distal compartment of fins and limbs (figure 4*a*) [51–53]. Importantly, this observation raises new questions about how the regulatory networks underpinning appendage formation evolved to expand the endoskeleton and reduce the fin-fold in tetrapods. Experimental manipulations in zebrafish have shown that overexpression of *HoxD13* [11], or rescue of the AER by serial AF removal [42] result in ectopic expansion of the endoskeleton. Similarly, knockdown of *Actinodin1/2* in zebrafish compromises the formation of the fin-fold and results in a distal gene expression profile consistent with digit polydactyly, a phenotype typical of early tetrapods [9]. Notably, these data recapitulate aspects of the fin-to-limb

transition, and in part support a trade-off between formation of the endoskeleton and fin-fold (*sensu* Thorogood's clock model [45]); however, the degree to which the morphogenetic dynamics of distal fin development in teleosts reflect those of other finned vertebrates remains poorly understood.

In paddlefish, endoskeletal and fin-fold compartments are specified early and expand throughout subsequent stages of development. During this process, components of the Shh/LIM/Gremlin/Fgf transcriptional network required for distal limb outgrowth and polarization are expressed within the fin-fold with a profile similar to that of the autopod (figure 4*b*). While future functional work is required to establish how members of this network interact during fin-fold development, our data suggest that Fgf-producing cells of the proximal AF maintain AER function following fin-fold formation and mediate transcription of genes associated with distal appendage identity, including those of the *HoxA/D* clusters [16,21,25, 52,67,81]. It is worth noting that the anuran *Eleutherodactylus* and urodeles lack a morphological AER [82,83], whereas certain lacertids and chelonians have a folded AER histologically comparable to the initial AF of fishes [40,82]. Such variation across phylogeny indicates that the signalling role of the distal appendage ectoderm is not coupled to local morphology [82], so long as the epithelium is adjacent to the underlying mesenchyme, a condition met in the proximal fin-folds of both paddlefish and catshark (figure 4*b*).

Recent fate-mapping studies in zebrafish have confirmed morphological descriptions to show that pectoral fin-bud mesenchyme derives from LPM [40,84]. Somitic mesoderm, by contrast, gives rise to the abaxial dorsal and ventral muscle masses [84,85], as well as cells that infiltrate the AER to induce ectodermal folding and AF outgrowth [45]. Our *Tbx5* and fate-mapping analyses for paddlefish demonstrate that a common LPM population—at least at the resolution of our injections—contributes to both the proximal fin and fin-fold mesenchyme, indicating this feature is not unique to teleosts [84]. While our DiI-labelled cells could not be tracked to differentiated anatomy, recent long-term labelling experiments in medaka demonstrate that LPM contributes to both the pectoral fin radials (endoskeleton) and late forming dermal rays (dermoskeleton), with no apparent contributions from neural crest ([84]; see also [86] and references therein). These results are consistent with data from tetrapods where LPM contributes to both the proximal limb and autopod, further supporting the conservation of early, distal appendage development between finned and limbed vertebrates.

Fossils fill the morphological gaps between extant taxa and provide the anatomical context for inferences about the development of basal lineages bracketing the fin-to-limb transition. Considering patterns of skeletal evolution in light of the data presented in this study, we suggest an interpretation of transitional morphologies that differs from the endoskeleton/dermoskeleton trade-off predicted by variations of the clock model [45]. In tetrapods, *HoxA13*-positive cells of the distal limb give rise to the bones of the autopod through a chondrogenic programme mediated by *Sox9* [19,81,87]. By contrast, in paddlefish and catshark, *HoxA13* is expressed in the fin-fold, forming a boundary with the more proximal *Sox9*-positive chondrogenic mesenchyme of the nascent fin radials (figure 4*a*). As mentioned above, zebrafish Cre-mediated maps of the *HoxA* enhancer e16 demonstrate labelling throughout dermal rays, with no labelling in the endoskeletal radials [53]. While long-term tracking of *Sox9* and *HoxA13* lineages is not currently tractable in basal actinopterygians or chondrichthyans, our expression analyses, together with these transgenic zebrafish results for late anatomy, demonstrate a striking contrast in the differentiation outcome of HoxA13 patterned cells between tetrapods and non-sarcopterygian fishes. Furthermore, these observations suggest that the novel acquisition of chondrogenic competency in the distal compartment of paired appendages—likely in the context of a conserved Shh/LIM/Gremlin/Fgf distal regulatory network—was a key step in elaborating the endoskeleton to form the bones of the autopod. These developmental changes are likely reflected in the dual differentiation outcomes (i.e. dermal and endoskeletal) of sarcopterygian fossils such as *Sauripterus* (figure 4*c*), and are supported by both the capacity for transgenic mice to activate zebrafish Actinodin enhancers in the autopod ectoderm [88], and transgenic zebrafish to activate Mouse HoxA11 AS enhancers in the fin-fold [80]. While not invoking anatomical homology between elements of the dermoskeleton and autopod, this scenario posits a deep regulatory homology [53,89] for the early distal appendage in gnathostomes.

Ethics. All experiments and animal care were in accordance with Kennesaw State University Institutional Animal Care and Use Committee (approved protocols 12-001, 16-001).

Data accessibility. GenBank accession numbers MF001289-1303.

Authors' contributions. F.J.T. and M.C.D. conceived the project and drafted the manuscript. S.M. provided support for chondrichthyan data. F.J.T., J.L.M. and E.H. performed experiments and imaging. G.K., S.T. and S.M.E.S. performed phylogenetic analyses. F.J.T., E.H. and M.C.D. generated figures. All authors gave final approval for publication.

Competing interests. The authors declare they have no conflict of interest.

Funding. This work was supported by grants from the National Science Foundation (IOS 1144965, 1656464 and MRI 1229237) to M.C.D. and instrumentation supplied by the Georgia Research Alliance.

Acknowledgements. We thank C. V. H. Baker and M. S. Modrell, University of Cambridge, UK for transcriptomic resource sharing, and Osage Catfisheries, Inc. for their dedication to paddlefish research. 12/101 antibody was from Developmental Studies Hybridoma Bank, created by the NICHD of the NIH and maintained at The University of Iowa, Department of Biology, Iowa City, IA 52242.

References

1. Clack JA. 2009 The fin to limb transition: new data, interpretations, and hypotheses from paleontology and developmental biology. *Annu. Rev. Earth Planet. Sci.* **37**, 163–179. (doi:10.1146/annurev.earth.36.031207.124146)
2. Schneider I, Shubin NH. 2013 The origin of the tetrapod limb: from expeditions to enhancers. *Trends Genet.* **29**, 419–426. (doi:10.1016/j.tig.2013.01.012)
3. Davis MC, Shubin N, Daeschler EB. 2004 A new specimen of *Sauripterus taylori* (Sarcopterygii, Osteichthyes) from the Famennian Catskill Formation of North America. *J. Vert. Paleontol.* **24**, 26–40. (doi:10.1671/1920-3)
4. Shubin NH, Daeschler EB, Jenkins FA. 2006 The pectoral fin of *Tiktaalik roseae* and the origin of the tetrapod limb. *Nature* **440**, 764–771. (doi:10.1038/nature04637)
5. Coates MI. 1996 The Devonian tetrapod *Acanthostega gunnari* Jarvik: postcranial anatomy, basal tetrapod interrelationships and patterns of skeletal evolution.

Trans. R. Soc. Edinburgh-Earth Sci. **87**, 363–421. (doi:10.1017/S0263593300006787)

6. Johanson Z, Burrow C, Warren A, Garvey J. 2005 Homology of fin lepidotrichia in osteichthyan fishes. *Lethaia* **38**, 27–36. (doi:10.1080/00241160510013141)
7. Onimaru K, Kuraku S, Takagi W, Hyodo S, Sharpe J, Tanaka M. 2015 A shift in anterior–posterior positional information underlies the fin-to-limb evolution. *Elife* **4**, e07048. (doi:10.7554/eLife.07048)
8. Onimaru K, Marcon L, Musy M, Tanaka M, Sharpe J. 2016 The fin-to-limb transition as the re-organization of a Turing pattern. *Nat. Commun.* **7**, 11582. (doi:10.1038/ncomms11582)
9. Zhang J, Wagh P, Guay D, Sanchez-Pulido L, Padhi BK, Korzh V, Andrade-Navarro MA, Akimenko MA. 2010 Loss of fish actinotrichia proteins and the fin-to-limb transition. *Nature* **466**, 234–237. (doi:10.1038/nature09137)
10. Davis MC, Dahn RD, Shubin NH. 2007 An autopodial-like pattern of Hox expression in the fins of a basal actinopterygian fish. *Nature* **447**, 473–476. (doi:10.1038/nature05838)
11. Freitas R, Gomez-Marin C, Wilson JM, Casares F, Gomez-Skarmeta JL. 2012 *Hoxd13* contribution to the evolution of vertebrate appendages. *Dev. Cell* **23**, 1219–1229. (doi:10.1016/j.devcel.2012.10.015)
12. Freitas R, Zhang GJ, Cohn MJ. 2007 Biphasic *Hoxd* gene expression in shark paired fins reveals an ancient origin of the distal limb domain. *PLoS ONE* **2**, e754. (doi:10.1371/journal.pone.0000754)
13. Gehrke AR *et al.* 2015 Deep conservation of wrist and digit enhancers in fish. *Proc. Natl Acad. Sci. USA* **112**, 803–808. (doi:10.1073/pnas.1420208112)
14. Woltering JM, Noordermeer D, Leleu M, Duboule D. 2014 Conservation and divergence of regulatory strategies at *Hox* loci and the origin of tetrapod digits. *PLoS Biol.* **12**, e1001773. (doi:10.1371/journal.pbio.1001773)
15. Zakany J, Duboule D. 2007 The role of *Hox* genes during vertebrate limb development. *Curr. Opin Genet. Dev.* **17**, 359–366. (doi:10.1016/j.gde.2007.05.011)
16. Andrey G, Montavon T, Mascrez B, Gonzalez F, Noordermeer D, Leleu M, Trono D, Spitz F, Duboule D. 2013 A switch between topological domains underlies *HoxD* genes collinearity in mouse limbs. *Science* **340**, 1234167. (doi:10.1126/science.1234167)
17. Berlivet S, Paquette D, Dumouchel A, Langlais D, Dostie J, Kmita M. 2013 Clustering of tissue-specific sub-TADs accompanies the regulation of *HoxA* genes in developing limbs. *PLoS Genet.* **9**, e1004018. (doi:10.1371/journal.pgen.1004018)
18. Mercader N, Selleri L, Criado LM, Pallares P, Parras C, Cleary ML, Torres M. 2009 Ectopic *Meis1* expression in the mouse limb bud alters P-D patterning in a Pbx1-independent manner. *Int. J. Dev. Biol.* **53**, 1483–1494. (doi:10.1387/ijdb.072430nm)
19. Scotti M, Kherdjemil Y, Roux M, Kmita M. 2015 A *Hoxa13*:Cre mouse strain for conditional gene manipulation in developing limb, hindgut, and urogenital system. *Genesis* **53**, 366–376. (doi:10.1002/dvg.22859)
20. Tabin C, Wolpert L. 2007 Rethinking the proximodistal axis of the vertebrate limb in the molecular era. *Genes Dev.* **21**, 1433–1442. (doi:10.1101/gad.1547407)
21. Cooper KL, Hu JKH, ten Berge D, Fernandez-Teran M, Ros MA, Tabin CJ. 2011 Initiation of proximal–distal patterning in the vertebrate limb by signals and growth. *Science* **332**, 1083–1086. (doi:10.1126/science.1199499)
22. Gonzalez-Lazaro M, Rosello-Diez A, Delgado I, Carramolino L, Sanguino MA, Giovinazzo G, Torres M. 2014 Two new targeted alleles for the comprehensive analysis of *Meis1* functions in the mouse. *Genesis* **52**, 967–975. (doi:10.1002/dvg.22833)
23. Mercader N, Leonardo E, Azpiazu N, Serrano A, Morata G, Martinez C, Torres M. 1999 Conserved regulation of proximodistal limb axis development by Meis1/Hth. *Nature* **402**, 425–429. (doi:10.1038/46580)
24. Rosello-Diez A, Arques CG, Delgado I, Giovinazzo G, Torres M. 2014 Diffusible signals and epigenetic timing cooperate in late proximo-distal limb patterning. *Development* **141**, 1534–1543. (doi:10.1242/dev.106831)
25. Rosello-Diez A, Ros MA, Torres M. 2011 Diffusible signals, not autonomous mechanisms, determine the main proximodistal limb subdivision. *Science* **332**, 1086–1088. (doi:10.1126/science.1199489)
26. Cunningham TJ, Duester G. 2015 Mechanisms of retinoic acid signalling and its roles in organ and limb development. *Nat. Rev. Mol. Cell Biol.* **16**, 110–123. (doi:10.1038/nrm3932)
27. Zeller R, Lopez-Rios J, Zuniga A. 2009 Vertebrate limb bud development: moving towards integrative analysis of organogenesis. *Nat. Rev. Genetics* **10**, 845–858. (doi:10.1038/nrg2681)
28. Zuniga A. 2015 Next generation limb development and evolution: old questions, new perspectives. *Development* **142**, 3810–3820. (doi:10.1242/dev.125757)
29. Benazet JD, Bischofberger M, Tiecke E, Goncalves A, Martin JF, Zuniga A, Naef F, Zeller R. 2009 A self-regulatory system of interlinked signaling feedback loops controls mouse limb patterning. *Science* **323**, 1050–1053. (doi:10.1126/science.1168755)
30. Farin HF, Ludtke THW, Schmidt MK, Placzko S, Schuster-Gossler K, Petry M, Christoffels VM, Kispert A. 2013 Tbx2 terminates Shh/Fgf signaling in the developing mouse limb bud by direct repression of *Gremlin1*. *PLoS Genet.* **9**, e1003467. (doi:10.1371/journal.pgen.1003467)
31. Khokha MK, Hsu D, Brunet LJ, Dionne MS, Harland RM. 2003 Gremlin is the BMP antagonist required for maintenance of Shh and Fgf signals during limb patterning. *Nat. Genet.* **34**, 303–307. (doi:10.1038/ng1178)
32. Merino R, Rodriguez-Leon J, Macias D, Ganan Y, Economides AN, Hurle JM. 1999 The BMP antagonist Gremlin regulates outgrowth, chondrogenesis and programmed cell death in the developing limb. *Development* **126**, 5515–5522.
33. Michos O, Panman L, Vintersten K, Beier K, Zeller R, Zuniga A. 2004 Gremlin-mediated BMP antagonism induces the epithelial–mesenchymal feedback signaling controlling metanephric kidney and limb organogenesis. *Development* **131**, 3401–3410. (doi:10.1242/dev.01251)
34. Panman L, Galli A, Lagarde N, Michos O, Soete G, Zuniga A, Zeller R. 2006 Differential regulation of gene expression in the digit forming area of the mouse limb bud by SHH and gremlin 1/FGF-mediated epithelial-mesenchymal signalling. *Development* **133**, 3419–3428. (doi:10.1242/dev.02529)
35. Scherz PJ, Harfe BD, McMahon AP, Tabin CJ. 2004 The limb bud Shh-Fgf feedback loop is terminated by expansion of former ZPA cells. *Science* **305**, 396–399. (doi:10.1126/science.1096966)
36. Verheyden JM, Sun X. 2008 An Fgf/*Gremlin* inhibitory feedback loop triggers termination of limb bud outgrowth. *Nature* **454**, 638–641. (doi:10.1038/nature07085)
37. Zuniga A, Haramis APG, McMahon AP, Zeller R. 1999 Signal relay by BMP antagonism controls the SHH/FGF4 feedback loop in vertebrate limb buds. *Nature* **401**, 598–602. (doi:10.1038/44157)
38. Tzchori I *et al.* 2009 LIM homeobox transcription factors integrate signaling events that control three-dimensional limb patterning and growth. *Development* **136**, 1375–1385. (doi:10.1242/dev.026476)
39. Bouvet J. 1974 Development of actinotrichia in pectoral fin of trout (*Salmo trutta* fario L.). *Archives D Anatomie Microscopique Et De Morphologie Experimentale* **63**, 79–96.
40. Grandel H, Schulte-Merker S. 1998 The development of the paired fins in the Zebrafish (*Danio rerio*). *Mech. Dev.* **79**, 99–120. (doi:10.1016/s0925-4773(98)00176-2)
41. Wood A, Thorogood P. 1984 An analysis of *in vivo* cell-migration during teleost fin morphogenesis. *J. Cell Sci.* **66**, 205–222.
42. Yano T, Abe G, Yokoyama H, Kawakami K, Tamura K. 2012 Mechanism of pectoral fin outgrowth in zebrafish development. *Development* **139**, 2916–2925. (doi:10.1242/dev.075572)
43. Mercader N. 2007 Early steps of paired fin development in zebrafish compared with tetrapod limb development. *Dev. Growth Diff.* **49**, 421–437. (doi:10.1111/j.1440-169x.2007.00942.x)
44. Masselink W *et al.* 2016 A somitic contribution to the apical ectodermal ridge is essential for fin formation. *Nature* **535**, 542–546. (doi:10.1038/nature18953)
45. Thorogood P. 1991 The development of the teleost fin and implications for our understanding of tetrapod limb evolution. *Dev. Patterning Vert. Limb* **205**, 347–354. (doi:10.1007/978-1-4615-3310-8_45)
46. Freitas R, Gomez-Skarmeta JL, Rodrigues PN. 2014 New frontiers in the evolution of fin development. *J. Exp. Zool. Part B Mol. Dev. Evol.* **322**, 540–552. (doi:10.1002/jez.b.22563)
47. Sordino P, Duboule D. 1996 A molecular approach to the evolution of vertebrate paired appendages. *Trends Ecol. Evol.* **11**, 114–119. (doi:10.1016/0169-5347(96)81089-5)

48. Yano T, Tamura K. 2013 The making of differences between fins and limbs. *J. Anat.* **222**, 100–113. (doi:10.1111/j.1469-7580.2012.01491.x)
49. Shubin NH, Davis MC. 2004 Modularity in the evolution of vertebrate appendages. In *Modularity in development and evolution* (eds G Schlosser, G Wagner), pp. 429–440. Chicago, IL: University of Chicago Press.
50. Woltering JM, Duboule D. 2010 The origin of digits: expression patterns versus regulatory mechanisms. *Dev. Cell* **18**, 526–532. (doi:10.1016/j.devcel.2010.04.002)
51. Ahn D, Ho RK. 2008 Tri-phasic expression of posterior *Hox* genes during development of pectoral fins in zebrafish: implications for the evolution of vertebrate paired appendages. *Dev. Biol.* **322**, 220–233. (doi:10.1016/j.ydbio.2008.06.032)
52. Tulenko FJ, Augustus GJ, Massey JL, Sims SE, Mazan S, Davis MC. 2016 *HoxD* expression in the fin-fold compartment of basal gnathostomes and implications for paired appendage evolution. *Sci. Rep.* **6**, 22720. (doi:10.1038/srep22720)
53. Nakamura T, Gehrke AR, Lemberg J, Szymaszek J, Shubin NH. 2016 Digits and fin rays share common developmental histories. *Nature* **537**, 225–228. (doi:10.1038/nature19322)
54. Ballard WW, Mellinger J, Lechenault H. 1993 A series of normal stages for development of *Scyliorhinus canicula*, the lesser spotted dogfish (*Chondrichthyes; Scyliorhinidae*). *J. Exp. Zool.* **267**, 318–336. (doi:10.1002/jez.1402670309)
55. Ballard WW, Needham RG. 1964 Normal embryonic stages of polyodon spathula (Walbaum). *J. Morphol.* **114**, 465–477. (doi:10.1002/jmor.1051140307)
56. Bemis WE, Grande L. 1992 Early development of the actinopterygian head.1. External development and staging of the paddlefish *Polyodon spathula*. *J. Morphol.* **213**, 47–83. (doi:10.1002/jmor.1052130106)
57. Modrell MS, Lyne M, Carr AR, Zakon HH, Buckley D, Campbell AS, Davis MC, Micklem G, Baker CVH. 2017 Insights into electrosensory organ development, physiology and evolution from a lateral line organ-enriched transcriptome. *eLife* **6**, e24197. (doi:10.7554/eLife.24197)
58. Edgar RC. 2004 MUSCLE: multiple sequence alignment with high accuracy and high throughput. *Nucleic Acids Res.* **32**, 1792–1797. (doi:10.1093/nar/gkh340)
59. Capella-Gutierrez S, Silla-Martinez JM, Gabaldon T. 2009 trimAl: a tool for automated alignment trimming in large-scale phylogenetic analyses. *Bioinformatics* **25**, 1972–1973. (doi:10.1093/bioinformatics/btp348)
60. Gascuel O. 1997 BIONJ: An improved version of the NJ algorithm based on a simple model of sequence data. *Mol. Biol. Evol.* **14**, 685–695. (doi:10.1093/oxfordjournals.molbev.a025808)
61. Modrell MS, Bemis WE, Northcutt RG, Davis MC, Baker CVH. 2011 Electrosensory ampullary organs are derived from lateral line placodes in bony fishes. *Nat. Commun.* **2**, 496. (doi:10.1038/ncomms1502)
62. Tulenko FJ, McCauley DW, MacKenzie EL, Mazan S, Kuratani S, Sugaharad F, Kusakabe R, Burke AC. 2013 Body wall development in lamprey and a new perspective on the origin of vertebrate paired fins. *Proc. Natl Acad. Sci. USA* **110**, 11 899–11 904. (doi:10.1073/pnas.1304210110)
63. Davis MC, Shubin NH, Force A. 2004 Pectoral fin and girdle development in the basal Actinopterygians *Polyodon spathula* and *Acipenser transmontanus*. *J. Morphol.* **262**, 608–628. (doi:10.1002/jmor.10264)
64. Sakamoto K, Onimaru K, Munakata K, Suda N, Tamura M, Ochi H, Tanaka M. 2009 Heterochronic shift in *Hox*-mediated activation of *sonic hedgehog* leads to morphological changes during fin development. *PLoS ONE* **4**, e5121. (doi:10.1371/journal.pone.0005121)
65. Fernandez-Teran M, Ros MA. 2008 The Apical Ectodermal Ridge: morphological aspects and signaling pathways. *Int. J. Dev. Biol.* **52**, 857–871. (doi:10.1387/ijdb.072416mf)
66. Mao JH, McGlinn E, Huang P, Tabin CJ, McMahon AP. 2009 Fgf-dependent Etv4/5 activity is required for posterior restriction of *sonic hedgehog* and promoting outgrowth of the vertebrate Limb. *Dev. Cell* **16**, 600–606. (doi:10.1016/j.devcel.2009.02.005)
67. Probst S *et al.* 2011 SHH propagates distal limb bud development by enhancing CYP26B1-mediated retinoic acid clearance via AER-FGF signalling. *Development* **138**, 1913–1923. (doi:10.1242/dev.063966)
68. Zhang Z, Verheyden JM, Hassell JA, Sun X. 2009 FGF-regulated Etv genes are essential for repressing *Shh* expression in mouse limb buds. *Dev. Cell* **16**, 607–613. (doi:10.1016/j.devcel.2009.02.008)
69. Lettice L, Hecksher-Sorensen J, Hill RE. 1999 The dominant hemimelia mutation uncouples epithelial–mesenchymal interactions and disrupts anterior mesenchyme formation in mouse hindlimbs. *Development* **126**, 4729–4736.
70. Ohuchi H *et al.* 1997 The mesenchymal factor, FGF10, initiates and maintains the outgrowth of the chick limb bud through interaction with FGF8, an apical ectodermal factor. *Development* **124**, 2235–2244.
71. Tanaka M, Munsterberg A, Anderson WG, Prescott AR, Hazon N, Tickle C. 2002 Fin development in a cartilaginous fish and the origin of vertebrate limbs. *Nature* **416**, 527–531. (doi:10.1038/416527a)
72. Ahn DG, Kourakis MJ, Rohde LA, Silver LM, Ho RK. 2002 T-box gene *tbx5* is essential for formation of the pectoral limb bud. *Nature* **417**, 754–758. (doi:10.1038/nature00814)
73. Gibson-Brown JJ, Agulnik SI, Silver LM, Niswander L, Papaioannou VE. 1998 Involvement of T-box genes *Tbx2-Tbx5* in vertebrate limb specification and development. *Development* **125**, 2499–2509.
74. Metscher BD, Takahashi K, Crow K, Amemiya C, Nonaka DF, Wagner GP. 2005 Expression of *Hoxa-11* and *Hoxa-13* in the pectoral fin of a basal ray-finned fish, *Polyodon spathula*: implications for the origin of tetrapod limbs. *Evol. Dev.* **7**, 186–195. (doi:10.1111/j.1525-142X.2005.05021.x)
75. Badugu A, Kraemer C, Germann P, Menshykau D, Iber D. 2012 Digit patterning during limb development as a result of the BMP-receptor interaction. *Sci. Rep.* **2**, 00991. (doi:10.1038/srep00991)
76. Jumlongras D *et al.* 2012 An evolutionarily conserved enhancer regulates *Bmp4* expression in developing incisor and limb bud. *PLoS ONE* **7**, e38568. (doi:10.1371/journal.pone.0038568).
77. Zhou W *et al.* 2013 Misexpression of *Pknox2* in mouse limb bud mesenchyme perturbs zeugopod development and deltoid crest formation. *PLoS ONE* **8**, e64237. (doi:10.1371/journal.pone.0064237)
78. Takamatsu N, Kurosawa G, Takahashi M, Inokuma R, Tanaka M, Kanamori A, Hori H. 2007 Duplicated *Abd-B* class genes in medaka *hoxAa* and *hoxAb* clusters exhibit differential expression patterns in pectoral fin buds. *Dev. Genes Evol.* **217**, 263–273. (doi:10.1007/s00427-007-0137-4)
79. Beccari L *et al.* 2016 A role for HOX13 proteins in the regulatory switch between TADs at the *HoxD* locus. *Genes Dev.* **30**, 1172–1186. (doi:10.1101/gad.281055.116).
80. Kherdjemil Y *et al.* 2016 Evolution of *Hoxa11* regulation in vertebrates is linked to the pentadactyl state. *Nature* **539**, 89–92. (doi:10.1038/nature19813)
81. Sheth R, Marcon L, Bastida MF, Junco M, Quintana L, Dahn R, Kmita M, Sharpe J, Ros MA. 2012 *Hox* genes regulate digit patterning by controlling the wavelength of a Turing-type mechanism. *Science* **338**, 1476–1480. (doi:10.1126/science.1226804)
82. Cooper LN, Armfield BA, Thewissen JGM. 2011 Fins and limbs: patterns of morphological variation during development. In *Epigenetics: linking genotype and phenotype in development and evolution* (eds B Hallgrímsson, BK Hall), pp. 238–255. Oakland, CA: University of California Press.
83. Gross JB, Kerney R, Hanken J, Tabin CJ. 2011 Molecular anatomy of the developing limb in the coqui frog, *Eleutherodactylus coqui*. *Evol. Dev.* **13**, 415–426. (doi:10.1111/j.1525-142X.2011.00500.x)
84. Shimada A *et al.* 2013 Trunk exoskeleton in teleosts is mesodermal in origin. *Nat. Commun.* **4**, 1639. (doi:10.1038/ncomms2643)
85. Neyt C, Jagla K, Thisse C, Thisse B, Haines L, Currie PD. 2000 Evolutionary origins of vertebrate appendicular muscle. *Nature* **408**, 82–86. (doi:10.1038/35040549)
86. Hall BK. 2014 Endoskeleton/exo (dermal) skeleton—mesoderm/neural crest: two pair of problems and a shifting paradigm. *J. Appl. Ichthyol.* **30**, 608–615. (doi:10.1111/jai.12522)
87. Raspopovic J, Marcon L, Russo L, Sharpe J. 2014 Digit patterning is controlled by a Bmp-Sox9-Wnt Turing network modulated by morphogen gradients. *Science* **345**, 566–570. (doi:10.1126/science.1252960)
88. Lalonde RL, Moses D, Zhang J, Cornell N, Ekker M, Akimenko MA. 2016 Differential *actinodin1* regulation in zebrafish and mouse appendages. *Dev. Biol.* **417**, 91–103. (doi:10.1016/j.ydbio.2016.05.019)
89. Shubin N, Tabin C, Carroll S. 2009 Deep homology and the origins of evolutionary novelty. *Nature* **457**, 818–823. (doi:10.1038/nature07891)